

# Effect of tides on solute flushing from a strait: imaging flow and transport in the East River with SF<sub>6</sub>

Theodore Caplow <sup>\*,1</sup>

Peter Schlosser <sup>1,2,3</sup>

David T. Ho <sup>2,3</sup>

Rica M. Enriquez <sup>4</sup>

## Abstract

In June 2003, 2 injections of ~3.9 mol sulfur hexafluoride (SF<sub>6</sub>) were made 8 days apart in the East River, a 25 km tidal strait, to observe solute mixing and dissipation. The first injection occurred at slack before flood, and the second at slack before ebb (flood = northward flow). Tidally synchronized surveys of the SF<sub>6</sub> tracer patch, supplemented by vertical profiles, were conducted by boat for 6 and 4 days following the flood and ebb injections, respectively. Residence times for the tracer-tagged water mass in the East River were estimated to be  $3.8 \pm 1.1$  days and  $1.7 \pm 0.5$  days for the flood and ebb injections, respectively, after correcting SF<sub>6</sub> inventories for losses of SF<sub>6</sub> from the water column by air-water gas exchange. The data indicate that the majority of East River solutes are transported to New York Harbor, and that tidal mixing dominates sub-tidal circulation with respect to solute transport. Surveys of the adjacent lower Hudson River revealed a northward-moving, intermediate layer of East River water. Our results suggest that tidal phasing of contaminant discharges in the East River could reduce environmental impacts, by increasing flushing rates and directing a greater fraction of material away from Long Island Sound.

\*Corresponding author phone: 212-854-0640; fax: 212-854-7081;  
email: tc144@columbia.edu.

<sup>1</sup>Department of Earth and Environmental Engineering,  
Columbia University, New York, NY, 10027,

<sup>2</sup>Lamont-Doherty Earth Observatory of  
Columbia University, Palisades, NY, 10964,

<sup>3</sup>Department of Earth and Environmental Sciences,  
Columbia University, New York, NY, 10027, and

<sup>4</sup>Whiting School of Engineering,  
Johns Hopkins University, Baltimore, MD, 21218

## Introduction

The aqueous mixing, transport, and dissipation of contaminant discharges affects the severity and location of environmental impacts from those contaminants. One prominent example from the waters surrounding New York City (the largest urban conglomeration in the U.S.) is the hypothesized connection between excess nutrients in sewage discharged from 6 treatment plants located along the East River (ER), a tidal strait, and hypoxic conditions in the bottom waters of adjacent Long Island Sound (LIS) (1,2,3). The ER and its adjoining creeks are the site of numerous other industrial discharges, combined sewer overflows, accidental oil spills, and environmental remediation sites (4,5,6).

Although studies that explicitly investigate the effects of tides on large-scale solute transport in bays and estuaries are not uncommon (e.g., 7,8), comparable studies in tidal straits are rare. Recent hydrodynamic investigations in the ER have used moored acoustic Doppler current profilers (ADCPs) coupled with numerical models (9,10,11). The former are limited by low spatial resolution, whereas the latter may not accurately represent mixing behavior unless calibrated by field data specifically tailored to quantify mixing. Deliberate releases of sulfur hexafluoride ( $\text{SF}_6$ ) have been used as a tracer in lakes, rivers, estuaries, and the open ocean (e.g., 12,13,14) to provide direct observational information on mixing and transport. High-resolution  $\text{SF}_6$  release experiments with spatial scales up to 100 km and temporal scales up to 2 weeks have been used in the Hudson-Raritan Estuary (15,16,17) to gain new insight into large-scale processes, and to provide data for model calibration and validation.

Here we describe an experiment investigating the transport of dissolved material discharged into the ER, with relevance to other tidal straits sharing similar characteristics (i.e., geometry, bathymetry, tidal strength, current velocities). By means of tracer injections and

subsequent sampling of tracer-tagged water, mixing patterns were visualized and rates of flushing were determined, with particular attention paid to effects of the tidal phase.

## **Study Location**

Not a true river, the East River is a 25 km long tidal strait connecting the west end of LIS, which opens to the Atlantic Ocean in the east, with Upper Bay (UB), which connects to the Atlantic Ocean via Raritan Bay (Figure 1). ER sediments are among the most contaminated in the Hudson-Raritan Estuary (4). The ER has been extensively dredged for navigational purposes. The mean depth is 13.7 m, the mean width of the navigable channel is 660 m, and the surface area and total volume (including contiguous bays) are  $\sim 20 \text{ km}^2$  and  $\sim 2.8 \times 10^8 \text{ m}^3$ , respectively.

We refer to locations on the ER by kilometers from  $\text{SF}_6$  injection (kmi), located roughly halfway between LIS and UB, opposite Sunken Meadow on Randall's Island. At this point, the narrower, lower ER, characterized by straight banks and swift currents, joins the wider, upper ER, characterized by indented shorelines, large bays, and slower currents. A positive kmi (or "upper ER") refers to a location between the injection point and LIS, while a negative kmi (or "lower ER") indicates a location between the injection point and UB. The Harlem River (11 km) connects the Hudson River with the ER at kmi  $-2.5$ .

Tides in western LIS (beyond kmi 11.5) lag tides at the Battery (kmi  $-13.5$ ) by nearly 4 h. This tidal lag governs the direction and velocity of the flow in the ER (where flow to the north is defined as the flood tide). Slack-before-flood (SBF) takes  $\sim 2$  h to propagate down the ER from north to south. For the next  $\sim 4$  h, the entire ER flows north (floods), after which slack-before-ebb (SBE) similarly propagates from north to south down the ER over a period of  $\sim 2$  h, followed by a  $\sim 4$  h period of southward (ebb) flow that completes the tidal cycle. Parts of the ER's bed are

highly irregular and narrow, particularly from the southern end of Roosevelt Island (kmi -6) to Sunken Meadow (kmi 0), leading to intense turbulence, longitudinal surface velocities as high as  $2.0 \text{ m s}^{-1}$ , and standing waves 1–2 m high on each tidal cycle.

**Sub-tidal circulation.** The direction and magnitude of the mean annual sub-tidal circulation in the ER are not firmly established. Blumberg and Pritchard (9) tabulate 8 different estimates, ranging from  $620 \text{ m}^3 \text{ s}^{-1}$  towards UB to  $1100 \text{ m}^3 \text{ s}^{-1}$  towards LIS. They estimate a flow of  $310 \text{ m}^3 \text{ s}^{-1}$  towards UB, based on a numerical model calibrated with two ADCPs located near opposite shores of the ER a few km from LIS (flow in the center of the channel was interpolated). Their model indicates vertically stratified flow between Hellgate (kmi -1.5) and LIS, with net flow toward LIS at the surface and towards UB at the bottom, and nonstratified flow south of Hellgate. Flow reversals (northward sub-tidal flow) on the weekly timescale are rare, according to the model: over a 144-day (April–August) model calibration period presented in detail, no flow reversals longer than 1 day are evident. A slightly lower flow of  $200 \text{ m}^3 \text{ s}^{-1}$  was reported from a similar study (10) (wastewater treatment plants in the ER were estimated to add an additional  $45 \text{ m}^3 \text{ s}^{-1}$  to this flow before reaching UB). These fluxes correspond to a southward sub-tidal circulation of  $2.5\text{--}3.8 \text{ km day}^{-1}$  (at kmi 0, cross-sectional area  $\sim 7000 \text{ m}^2$ ).

Blumberg and Pritchard (9) conclude that the magnitude of damage to LIS from ER pollution inputs depends upon the strength and direction of the sub-tidal circulation in the ER. A similar emphasis on residual circulation as a primary determinant of contaminant fate has been made for LIS (18). Turekian et al. (19) have taken a different approach, using a radium isotope signature from the ER to directly estimate the flux rate of tracer-tagged water from the ER to LIS at  $1300\text{--}3500 \text{ m}^3 \text{ s}^{-1}$  (this figure does not represent residual circulation, because the return flow of water from LIS to the ER is unspecified).

**Tidal Ranges.** Spring tides occurred at the Battery on June 13 (4 days before the flood injection) and on June 27 (2 days after the ebb injection). The mean tidal ranges at this station during the 5 days following the flood and ebb injections were approximately 1.3 m and 1.2 m, respectively, and the long-term mean is 1.38 m. Typical peak tidal surface velocities (determined from repeated field observations at center-channel of boat drift via GPS) of  $1.8 \text{ m s}^{-1}$  and  $0.8 \text{ m s}^{-1}$  suggest net surface tidal excursions of 26 km and 11 km, in the lower and upper halves of the ER, respectively, assuming a sinusoidal velocity distribution through time. These estimates are in good agreement with those published in the literature (9).

**Precipitation.** Two  $\text{SF}_6$  injections were carried out during the present experiment. Precipitation (measured at La Guardia Airport, 3 km from the injection point) during the 5 days following the first (“flood”) injection was heavy, totaling 5.7 cm. Precipitation during the 5 days following the second (“ebb”) injection was light, totaling 0.1 cm. The long-term (30 y) mean precipitation for 5 days in June is 1.5 cm, which is also the mean 5-day rainfall on an annual basis. However, tributary flows into the ER are insignificant in comparison to the tidal fluxes, and Blumberg and Pritchard (9) found that the freshwater flow in the Hudson River (a proxy for precipitation) was essentially uncorrelated (correlation coefficient of 0.15) with ER residual circulation in their model.

## Methods

An automated, high-resolution,  $\text{SF}_6$  measurement system (15) was used during the experiment, including a submerged pump, a flow-through membrane contactor to extract gases, and a gas chromatograph equipped with an electron capture detector (GC-ECD). A new chromatographic inlet system with twin analytical columns was designed and installed, enabling a continuous

measurement interval of 60 s with a single GC-ECD, thereby doubling the temporal and spatial resolution achieved previously with this system. Vertical profiles of salinity (conductivity) and temperature were collected using a CTD sonde (Seabird SBE 19plus) at selected daily stations, and twice along a 30-km longitudinal section (with center-channel stations spaced at 1.9 km) through the ER, UB, and LIS.

**Tracer injection.** On the morning of June 17, 2003, SF<sub>6</sub> was bubbled through a weighted coil of perforated hose (7 m long, 0.6 cm ID, 150 μm pores) that was towed twice across the navigable channel at a depth of 10 m ± 1 m (monitored by pressure sensor) at kmi 0. (Figure 1). The injection (“flood injection”) lasted 20 ± 0.5 min and coincided with SBF at Hellgate (kmi – 1.5) as predicted by the Xtide software program (20). A longitudinal survey several hours after this injection indicated that 3.9 ± 0.7 mol of SF<sub>6</sub> dissolved into the water column. A second injection, identical in technique, was conducted on the morning of June 25 at the same location and depth. This second injection (“ebb injection”) coincided with SBE, rather than SBF. A variable area tube flow meter and stopwatch were used to ensure that both injections used the same SF<sub>6</sub> flow rate, and had the same duration. It was assumed that the same amount of SF<sub>6</sub> (±10%) dissolved in the water during the second injection as during the first injection (a complete independent survey was not possible in this case, because part of the SF<sub>6</sub> patch entered UB within hours of the injection).

**Sampling strategy.** The SF<sub>6</sub> patch from the flood injection was tracked for 6 consecutive days (days 1F–6F; the flood injection day is designated as day 0F; an incomplete survey from day 7F was discarded). Each day, longitudinal surveys were completed from LIS to UB through the center of the deepwater channel in the ER, with a sampling depth of 1.2 m and a typical sample spacing of 200 m (for comparison, the preliminary survey on day 0F indicated a peak

width of ~5000 m for the SF<sub>6</sub> patch). The survey on day 1F was timed so that the boat passed the injection point exactly 1 tidal day (= 2 tidal cycles ≈ 25 h) after the injection. Each subsequent survey was retarded by an additional tidal day, so that the complete set of longitudinal surveys were all tidally synchronized; i.e. the boat passed the injection point at the same state of the tide (± 3 min), regardless of the day. The precision over the rest of the ER was ± 10 min (i.e., the boat passed each point on the ER at the same state of the tide, regardless of the day, within this margin of error). The lengths of the tidal days were determined from Xtide (20).

The SF<sub>6</sub> patch from the ebb injection was tracked for 4 consecutive days (days 1E–4E; the ebb injection day is designated 0E and coincides with day 8F; an incomplete survey from day 5E was discarded). All the longitudinal surveys were again performed from LIS to UB, but in this case they were synchronized to occur at the same state of the tide as the ebb injection (± 3 min near kmi 0; ± 10 min for the entire ER). Flood injection surveys required 2.7 h for transit of the entire ER, while ebb injection surveys covered the same distance in 1.6 h.

In addition to the two sets of synchronized longitudinal surveys, additional surface sampling was conducted during 1 or more days in UB, LIS, Raritan Bay, the Hudson River, and the Harlem River. 26 vertical SF<sub>6</sub> profiles were obtained throughout the study area, distributed over 8 different days of the experiment, with an average resolution of 4 depth levels and duplicate samples at each depth.

**Background concentrations of SF<sub>6</sub>.** The expected concentration of SF<sub>6</sub> in New York Harbor at solubility equilibrium with the local atmosphere is ~2 fmol L<sup>-1</sup>, given a local atmospheric mixing ratio of ~10 ppt (21, 22) and an Ostwald solubility coefficient of 4.9 x 10<sup>-3</sup> at 25 °C and a salinity of 20 (23). The study area was sampled for SF<sub>6</sub> (on an ebb tide) the day before the first injection. Mean levels in LIS, the upper ER, the lower ER, and UB were

approximately 150, 400, 600, and 300 fmol L<sup>-1</sup>, respectively (Figure 4). These values indicate significant addition of SF<sub>6</sub> to the waters in New York Harbor, from unidentified sources.

## Results

**Density structure.** As a result of swift currents and irregular bathymetry, the vertical density structure in the central and lower ER is generally very weak (Figure 2), characterized by total surface to bottom density differences < 0.5 kg m<sup>-3</sup>. Towards both ends of the ER, an estuarine structure becomes evident, and surface/bottom differences increase to 2–3 kg m<sup>-3</sup>. Surface salinity in the lower and upper halves of the ER was 17–21, and 21–23, respectively, over the study period. The mean surface salinity for the entire ER was 19.9.

**SF<sub>6</sub> in the East River.** A series of daily maps of SF<sub>6</sub> concentrations enables direct visualization of tracer spreading (Figure 3). SF<sub>6</sub> concentration versus kmi was compiled in a single graph for the flood injection (Figure 4), and a second set of plots explores the differences between the flood and ebb injections (Figure 5). Maximum SF<sub>6</sub> concentrations on days 1F and 1E were ~20000 fmol L<sup>-1</sup>, and by days 4F and 4E, maximum concentrations were 4000 and 1350 fmol L<sup>-1</sup>, respectively. The increasing spread between flood and ebb tide maxima indicate significantly faster flushing of the ebb tide injection.

The persistent and stationary peaks and valleys in the longitudinal SF<sub>6</sub> distribution indicate areas where tidal action has inserted water that is lower or higher in SF<sub>6</sub> into the main ER water mass, most likely from bays within the river or in the western end of LIS. A similar pattern was observed in Newark Bay, using the same SF<sub>6</sub> technique (17). The spatial scale of these valleys gives some indication of the scale of macroscopic tidal eddies in this system. In the upper ER, where these features are most evident, this scale ranges from ~1 km, for the series of

small but persistent peaks and valleys from kmi 4 to kmi 11, to ~5 km, for the large valley at kmi 4. These features are less evident following the ebb injection, indicating that the ER is more smoothly mixed longitudinally at this state of the tide (SBE).

Data from 12 vertical SF<sub>6</sub> profiles in the ER were plotted by region (Figure 6). In the lower ER, the vertical tracer gradient, although somewhat variable, is weak (surface/bottom ratios of SF<sub>6</sub> were typically within 25% of unity). The upper ER displays a stronger vertical tracer gradient, with mean surface/bottom ratios around 3.0. Close agreement in this region between flood and ebb profiles, taken at opposite tidal phases, suggests that the vertical structure in this part of the river is not strongly influenced by the tidal phase.

Measured SF<sub>6</sub> concentrations below 1000 fmol L<sup>-1</sup> approach the background levels and should be treated with appropriate caution; throughout the experiment, this condition was limited to the southern extreme of the ER (south of kmi -12) and to UB, except for day 4E, when SF<sub>6</sub> concentrations were between 600 and 1200 fmol L<sup>-1</sup> in much of the ER.

**Mass inventories.** Bathymetry was digitized from NOAA charts (#12335, #12339, #12366) using a longitudinal resolution of 500 m and a transverse resolution of ~100 m. Vertical SF<sub>6</sub> profiles in the ER, taken at a variety of tidal states, were plotted versus kmi (Figure 7) and interpolated to construct an index of correction factor versus kmi (correction factor = the expected ratio of surface concentration, which was measured, to vertical average concentration, which is needed for a mass inventory). The mean correction factor for the entire ER is  $0.77 \pm 0.18$ . Due to the tidal synchronization of the longitudinal surveys, any errors in the index of correction factors will have a systematic effect on the mass inventories (to the extent that the vertical tracer structure is relatively invariant on the sub-tidal timescale), and therefore a minimal impact on the calculated flushing times.

Tracer gradients in the transverse (cross-channel) direction were also considered. In the lower ER, the predictive relationships of Fischer et al. (24) indicate that the narrow width and swift currents are adequate to ensure complete transverse mixing (center/edge concentration ratios  $\geq 0.90$ ) of a point injection 10 h after injection (the actual injection was along a transverse line, further accelerating mixing). The upper ER contains a number of deep bays and indentations, where the transverse distribution of tracer was studied on day 1F. No significant transverse gradients were observed between the center and the edges of the main channel, but mean tracer concentrations at the ends of the deeper bays (Flushing Bay and Riker's Island Channel) were approximately 20% lower than those in the main channel. Time was not available to survey these bays on subsequent days. Throughout the study, tracer concentrations recorded in those sections of the daily longitudinal survey that include bays were reduced by 10% before being added to the mass inventory, to account for the transverse gradient. (This approximation, adopted for simplicity, assumes a linear relationship between concentration and cross-sectional area, along an axis from the main channel into the bays). These sections constitute 9% of the ER volume, so the total transverse correction applied to the mass inventories is <1%.

The mass inventory from each day was used to calculate the center of mass (COM) in the ER. The daily movement of the COM was plotted versus time (Figure 8). The mean displacement of the COM was northward by  $0.4 \pm 0.5 \text{ km day}^{-1}$  and  $2.0 \pm 1.4 \text{ km day}^{-1}$  for days 0F-4F and 0E-4E, respectively. The distribution of SF<sub>6</sub> from the background survey, which yielded a total of  $0.17 \pm 0.03 \text{ mol}$  of SF<sub>6</sub> in the ER (4% of the amount injected), was subtracted before calculating the mass inventories and COM. However, the variability of the background is unknown, causing the error estimates for the mass inventories and COM to double.

Throughout the study, tracer was surveyed 15-20 km beyond the ends of the ER in both directions, but with insufficient resolution to estimate mass inventories. Nonetheless, the data strongly suggest that UB receives the majority of ER solutes, because (a) the flushing rate for the ebb tide injection, which occupied that part of the ER water mass most exposed to UB, was about twice as fast as the flushing rate for the flood tide injection; and (b) the northward movement of the COM, manifested after both injections despite the expected southward sub-tidal circulation, suggests that tracer is being removed much more quickly from the lower end of the river (i.e., from the southern flank of the tracer peak).

**Harlem River.** The Harlem River was longitudinally surveyed 4 times (Figure 9). For the flood injection, mean SF<sub>6</sub> concentration in the Harlem River was 77 fmol L<sup>-1</sup> (below ER background levels) on day 1F, rising to 440 fmol L<sup>-1</sup> by day 4F. For the ebb injection, despite much faster flushing from the ER, mean concentrations in the Harlem River were much higher than for the flood injection: 2700 fmol L<sup>-1</sup> on day 1E, and 820 fmol L<sup>-1</sup> on day 4E. These comparisons understate the true contrast, because the flood injection surveys were taken closer to SBE (when the Harlem River would contain a maximum amount of tracer-tagged ER water), whereas the ebb injection surveys were taken closer to SBF (when the Harlem River would be maximally refreshed with untagged Hudson River water). The tidal excursion in the Harlem River is ~11 km, based on observed velocities.

**East River SF<sub>6</sub> plume in the Hudson River.** Vertical SF<sub>6</sub> profiles in the Hudson River ranging from the Battery (at the tip of Manhattan) to the George Washington Bridge (15 km north of the Battery) indicate a three-layered structure (Figure 10). The middle of the water column, at a depth of 5–9 m, manifests SF<sub>6</sub> concentrations about twice those at the top or bottom. This intermediate layer, with a salinity of 16-22, is the best match for ER water (salinity

~20). Thus, the vertical profiles suggest that water from the ER is carried up the Hudson River in a layer beneath the fresher water flowing downstream at the surface, but above the more saline water pushing upstream along the bottom (this classic “salt wedge” pattern is present in the Hudson River up to 100 km north of the Battery, depending upon conditions). For the profiles following the ebb injection (Figure 10b), tracer transport through the Harlem River may have been significant.

Vertical profiles of SF<sub>6</sub> concentrations within a few km of the Hudson River’s mouth, taken 2–4 days following the flood injection, are nearly invariant (Figure 10a), indicating that the SF<sub>6</sub> found in the water column at this location (maximum concentration: 550–650 fmol L<sup>-1</sup>) may reflect the background detected in the lower ER (~600 fmol L<sup>-1</sup>) rather than the injection. If so, some two-thirds of the Hudson River at this point appears to originate in the ER (these 3 profiles were taken at or near high tide; different tidal phases may yield different results).

## Discussion

The decay of the ER SF<sub>6</sub> mass inventory was plotted versus tidal day for each injection (Figure 11a). After 4 days (on days 4F and 4E), approximately 13% and 2% of the flood and ebb tide injections, respectively, remained in the ER. The day 4E inventory was not significantly different from the background observed prior to the injection.

**Correction for air-water gas transfer.** The gas transfer velocity,  $k$ , may be defined as follows (25):

$$k = \lambda_g h \left( \frac{\bar{c}}{c_s} \right) \quad (1)$$

where  $\bar{c}$  and  $c_s$  are aqueous gas concentrations, averaged over the water column and measured at the surface, respectively,  $\lambda_g$  is the first-order gas transfer loss rate for the water column, and  $h$  is

the mean water depth. Gas transfer velocities for each tidal day were estimated by examining correlations from the literature between  $k$  and  $U_{10}$  (wind speed at 10 m height), and between  $k$  and  $v$  (mean river flow velocity). The effect of rainfall on gas exchange was neglected, because application of the relationship between  $k$  and rain rate proposed by Ho et. al. (26) produced values of  $k$  that were only ~3% of values produced using other methods.

Values for the parameters  $\bar{c}/c_s$  and  $v$  were sharply different in the upper ER and in the lower ER. For the flood injection,  $k$  was estimated based on mean conditions in the upper ER, because the mean position of the SF<sub>6</sub> peak from this injection was in the upper ER. Conversely, for the ebb injection,  $k$  was estimated based on mean conditions in the lower ER, because the mean position of the SF<sub>6</sub> peak from this injection was in the lower ER.

Although quadratic relationships between  $k$  and  $U_{10}$  derived for the ocean (27,28) were considered, the relationship of Clark et al. (29), developed primarily from gas exchange data collected with dual deliberate tracers (SF<sub>6</sub> and <sup>3</sup>He) on the Hudson-Raritan Estuary, seems the most appropriate for the ER:

$$k(600) = 0.24 (U_{10})^2 + 2.0 \quad (2)$$

where  $U_{10}$  is measured in m s<sup>-1</sup> and  $k(600)$ , expressed in cm h<sup>-1</sup>, is the gas transfer velocity normalized to a Schmidt number,  $Sc$ , of 600. ( $Sc$  is the kinematic viscosity of water divided by the aqueous diffusivity of a gas, and  $Sc = 600$  corresponds to CO<sub>2</sub> in fresh water at 20 °C). Hourly wind speeds at La Guardia Airport were applied to Equation (2), yielding a mean  $k(600)_{\text{wind}}$  for each day, averaging  $5.6 \pm 1.1$  cm h<sup>-1</sup> and  $5.7 \pm 1.1$  cm h<sup>-1</sup>, following the flood (6 days) and ebb (4 days) injections, respectively.

Study of the relationship between river flow and  $k$  is less well developed, particularly for tidal straits, but the relatively high  $v$  and rough bathymetry in the ER prompts consideration of

theoretically predicted relationships between  $k$  and  $v$  in rivers as a function of depth, collected and summarized by Raymond and Cole (30) for the range  $0.1 \text{ m s}^{-1} < v < 1.0 \text{ m s}^{-1}$ . These relationships were applied (extrapolating where necessary) separately to the upper half ( $h = 13.6 \text{ m}$ ,  $v = 1.2 \text{ m s}^{-1}$ ) and to the lower half ( $h = 13.9 \text{ m}$ ,  $v = 0.5 \text{ m s}^{-1}$ ) of the ER, yielding  $k(600)_{\text{flow}}$  of  $3.2 \pm 0.8 \text{ cm h}^{-1}$  and  $6.2 \pm 1.5 \text{ cm h}^{-1}$  for the flood and ebb injections, respectively.

A method for combining estimates of  $k$  derived separately from wind forcing and from current forcing has not been established, so the wind forcing was taken as the lower bound, and the linear addition of the two forcings was taken as an upper bound. The mean value between these bounds was chosen as an estimate of  $k(600)$  (with the expected error specified by the range), yielding mean values of  $7.2 \pm 1.6 \text{ cm h}^{-1}$  and  $8.8 \pm 3.1 \text{ cm h}^{-1}$  for the flood and ebb injections, respectively.

Based on mean conditions in the ER during the study ( $18.7 \text{ }^\circ\text{C}$ , salinity = 19.9),  $Sc$  for  $\text{SF}_6$  was calculated (31) as 1043. Through the relationship  $k \propto Sc^{-0.5}$  (32), daily  $k(\text{SF}_6)$  values were derived from  $k(600)$ , and used in Equation (1) to yield daily estimates of  $\lambda_g$ , representing the expected loss rates of  $\text{SF}_6$  from the ER if gas exchange were acting alone. Values of  $\bar{c}/c_s$  of  $0.64 \pm 0.23$  and  $0.95 \pm 0.14$  were used for the flood and ebb injections, respectively, representing the mean vertical correction factors for the upper ER and lower ER (Figure 7). Mean values of  $\lambda_g$  were  $0.15 \pm 0.03 \text{ day}^{-1}$  and  $0.12 \pm 0.04 \text{ day}^{-1}$  for the flood and ebb injections, respectively, corresponding to 36% and 19% of the total tracer lost from the ER following these injections.

The mass inventories were recalculated for each day with the estimated gas losses restored, yielding a decay series corresponding to the predicted behavior of soluble, non-volatile materials (Figure 11b). The positive and negative error estimates reported for  $\lambda_g$  were

systematically applied to the inventory estimates to yield scenarios corresponding to the upper and lower bounds on  $k$ . These bounds (together with other sources of uncertainty) are represented by the error bars in Figure 11b, indicating that the uncertainty in  $k$  does not materially affect the comparison of flushing times for the ebb and flow injections. Separate first-order exponential decay curves were fit to the data for the flood injection (6 days of surveys) and for the ebb injection (4 days of surveys). Although the decay of the ebb injection is not closely represented by an exponential curve, the inventory observed on days 3E and 4E is predicted reasonably well by the function shown.

Mean residence times (the time required for the tracer mass in the ER to decline by a factor of  $1/e$ ) were  $3.8 \pm 1.1$  days and  $1.7 \pm 0.5$  days for the flood and ebb injections, respectively, using the curve fits shown. The sub-tidal flow estimated in the literature (9,10) yields a significantly longer residence time (5.2–8.1 days), indicating that solute flushing from these waters is dominated by tidal mixing, and not by residual circulation. For comparison, the rate of ER flux to LIS calculated from radium isotopes (19) yields a residence time of 0.9–2.5 days.

The decay patterns for both injections are monotonic, but the decay rates are not as constant as those observed for the tidal flushing of Newark Bay (17), a 14 km<sup>2</sup> water body north of Staten Island that connects with UB. The rapid pace of flushing, very long tidal excursion of the lower ER, and highly indented shoreline of the upper ER may all contribute to this unsteadiness, the source of which remains undetermined. None of these features were found in Newark Bay.

The general dominance of large-scale tidal transfer in the flushing of solutes from the ER echoes an analogous situation observed in the Kill van Kull (17), a similar tidal strait terminating

on the opposite side of UB, where the key factors determining the rate of solute transport appeared to be the length of the tidal excursion relative to the length of the strait, and the relative degree of dispersive mixing taking place at either end of the strait. Thus, the accelerated flushing rates in the lower ER, when compared with the upper ER, are likely due to a substantially longer tidal excursion in the former, assisted by a stronger mixing regime in UB than exists in LIS.

**Implications for wastewater management.** In the central reaches of the ER, solutes discharged at or near SBE disappear from the river twice as fast as solutes discharged at or near SBF. The evidence suggests that this difference in flushing time reflects a difference in partitioning between LIS and UB as solute receptors for the ER, and that a smaller fraction of material discharged near SBE is ultimately released to LIS. (This partitioning result is expected to hold for discharges in almost any part of the ER, although further experiments are needed to verify that hypothesis). If this conclusion is correct, then the impact on LIS of wastewater discharged in the ER could be substantially reduced by tidally phasing these discharges to favor SBE (e.g., by suspending discharge from 2–3 h before SBF until 2–3 h after SBF).

Other contaminated discharges to the ER, particularly those with lower fluxes and higher toxicity, and/or those for which residence time in the ER is a factor, are also well suited to tidal phasing. Examples include heavy metals, PCB's, dioxins, and similar particle-bound toxins with the potential to settle into the sediment bed. With regard to flushing toxins out of the ER *per se* (as opposed to directing them away from LIS), it would be desirable to determine the “break-even” point (if such a point exists) in the upper ER, at which ebb flushing and flood flushing proceed at an equal pace.

The use of discharge holding tanks to reduce spikes in contaminant concentrations at times of slack water in estuaries has been previously proposed (33), and the theoretical

implications of various temporal patterns of contaminant discharge into estuaries have been explored (34). However, the potential for phased discharge to affect the direction of net solute transport in tidal straits, and in the ER in particular, appears to be underexamined. Evaluation of the relative merits and costs of phased discharge vs. other remediation activities, such as the planned construction of nitrogen-reducing equipment at treatment plants along the ER, lies beyond the scope of this contribution.

**Transport of ER water into the Hudson River.** The extent of the submerged ER plume in the Hudson River, where it was distinctly identified up to 15 km north of the Battery, demonstrates that surface measurements of water quality in estuaries may overlook remotely generated, upstream-moving contaminant plumes.

Tracer appears to have reached the Hudson River via the Harlem River within the first day following the ebb injection (Figure 9). By contrast, it appears unlikely that significant tracer was transported to the Hudson River via this path following the flood injection. This difference may have significant implications in cases where Hudson River ecological endpoints are the focus. In general, the transport of contaminated water from the ER (and from Newark Bay) to the Hudson River is under-examined. Further examination of this phenomenon would be best achieved by a combination of tracers, including salinity, SF<sub>6</sub>, and an isotope, biological marker, or anthropogenic compound that could definitively identify source waters.

**Outlook.** The short SF<sub>6</sub> measurement interval of the deployed system produces high-resolution quantitative and qualitative imaging of transport processes. This imaging reveals the Hudson-Raritan Estuary as an interconnected system, within which solutes are exchanged in a complex pattern determined by the action of tidal forcing on local geometry. Vital data is also provided for the calibration and validation of numerical hydrodynamic models, which may then

be applied at relatively low cost to aid navigation, predict contaminant pathways, simulate consequences from natural and anthropogenic disasters, etc.

Future work of this kind in the ER, and in similar straits, would benefit from multiple sampling platforms (e.g. one stationed at each end of the river, to record net tracer flux), repeated experiments under different forcing from tides, runoff, and wind, and a long-term survey of background sources of SF<sub>6</sub>.

This experiment is the first of its kind that we are aware of to use a tidally synchronized sampling scheme. The synchronization technique, combined with serial dual injections at opposite states of the tide, appears to be an effective tool for determining the importance of tidal phase on the fate of contaminant discharges and natural solutes (e.g. fish larvae). More broadly, this study highlights the potential for an increasingly sophisticated approach to coastal water quality management, in which tidal phase is considered in the measurement of toxin levels, and discharge permits are granted for selected times.

## **Acknowledgements**

We thank F. Hellweger, X. Liu, and H. Roth for assistance in the field, B. Huber for preparation of the CTD, J. Lipscomb at Riverkeeper for expert handling of the research vessel, and E. Wei at NOAA's Office of Coast Survey for preliminary flow forecasts. We also thank J. Clark for suggesting that a study of East River flushing at different tidal states might yield interesting implications for wastewater management. Streamflow and tide data were obtained from the USGS website <<http://water.usgs.gov>>, and tide predictions were obtained from the LDEO emulation of Xtide. Wind and rain data at LaGuardia airport was obtained from NOAA/NCDC. Remote SF<sub>6</sub> mixing ratios were obtained from NOAA/CMDL. Funding was provided by a generous gift from the Dibner Fund, by the Lamont Investment Fund, and by the National Science Foundation through a Graduate Fellowship (TC). LDEO contribution no. xxxx.

## **Literature Cited**

- (1) O'Shea, M. L.; Brosnan, T. M. *Estuaries* **2000**, *23*, 877-901.
- (2) Anderson, T. H.; Taylor, G. T. *Estuaries* **2001**, *24*, 228-243.

- (3) U. S. Environmental Protection Agency *2001 Long Island Sound Study CCMP Implementation Tracking Report*; U.S. Environmental Protection Agency: Stamford, CT, 2001.
- (4) Wolfe, D. A.; Long, E. R.; Thursby, G. B. *Estuaries* **1996**, *19*, 901-912.
- (5) Wakeman, T. H.; Themelis, N. J. *J. Hazard. Mater.* **2001**, *85*, 1-13.
- (6) Protopapas, A. L. *Water Resour. Manage.* **1999**, *13*, 133-151.
- (7) Gargett, A. E.; Stucchi, D.; Whitney, F. *Estuar. Coast. Shelf Sci.* **2003**, *56*, 1141-1156.
- (8) Das, P.; Marchesiello, P.; Middleton, J. H. *Mar. Freshw. Res.* **2000**, *51*, 97-112.
- (9) Blumberg, A. F.; Pritchard, D. W. *J. Geophys. Res.* **1997**, *102*, C3, 5685-5703.
- (10) Blumberg, A. F.; Khan, L. A.; St. John, J. P. *J. Hydraul. Eng.* **1999**, *125*, 799-816.
- (11) Wei, E.; Chen, M. *Hydrodynamic Model Development for the Port of New York/New Jersey Water Level and Current Nowcast/Forecast Model System*; Nat. Oceanic and Atmos. Admin., Office of Coast Survey: 2001, technical report NOS-OCS-12, 53 pp.
- (12) Ledwell, J. R.; Watson, A. J.; Law, C.S. *Nature* **1993**, *364*, 701-703.
- (13) Maiss, M.; Ilmberger, J.; Zenger, A.; Münnich, K.O. *Aquatic Sciences* **1994**, *56*, 307-328.
- (14) Clark, J. F.; Schlosser, P.; Stute, M.; Simpson, H. J. *Environ. Sci. Technol.* **1996**, *30*, 1527-1532.
- (15) Ho, D. T.; Schlosser, P.; Caplow, T. *Environ. Sci. & Technol.* **2002**, *36*, 3234-3241.
- (16) Caplow, T.; Schlosser, P.; Ho, D. T. Dispersion, advection, and gas transfer in a dammed channel: high-resolution SF<sub>6</sub> tracer study of the upper Hudson River. *J. Environ. Eng.*, Accepted for publication.
- (17) Caplow, T.; Schlosser, P.; Ho, D. T.; Santella, N. Transport dynamics in a sheltered estuary and connecting tidal straits: SF<sub>6</sub> tracer study in New York Harbor. *Environ. Sci. & Technol.*, In press.
- (18) Viera, M. E. C. *Estuaries* **2000**, *23*, 199-207.
- (19) Turekian, K. K.; Tanaka, N.; Turekian, V. C.; Torgersen, T.; DeAngelo, E. C. *Cont. Shelf Res.* **1996**, *16*, 863-873
- (20) Flater, D. *Linux Journal* **1996**, *32*, 51-57
- (21) Ho, D. T.; Schlosser, P. *Geophys. Res. Lett.* **2000**, *27*, 1679-1682.
- (22) Santella, N.; Ho, D. T.; Schlosser, P.; Stute M. *Environ. Sci. Technol.*, **2003**, *37*, 1069-1074.
- (23) Bullister, J. L.; Wisegarver, D. P.; Menzia, F. A. *Deep-Sea Research I* **2002**, *49*, 175-187.
- (24) Fischer, H. B.; List, E. J.; Imberger, J.; Koh, R. C. Y.; Brooks, N. H. *Mixing in inland and coastal waters* Academic Press: New York, NY, 1979.
- (25) Ledwell, J. R. Ph. D. Dissertation, Harvard University, 1982.
- (26) Ho, D. T.; Bliven, L. F.; Wanninkhof, R. ; Schlosser, P. *Tellus* **1997**, *49B*, 149-158.
- (27) Nightingale, P. D.; Malin, G.; Law, C. S.; Watson, A. J.; Liss, P. S.; Liddicoat, M. I.; Boutin, J.; Upstill-Goddard, R. C. *Global Biogeochem. Cy.* **2000**, *14*, 373-387
- (28) Wanninkhof, R. *J. Geophys. Res.* **1992**, *97*, 7373-7382.
- (29) Clark, J. F.; Schlosser, P.; Simpson, H. J.; Stute, M.; Wanninkhof, R.; Ho, D. T. In *Air-Water Gas Transfer, Proceedings of the Third International Symposium on Air-Water Gas Transfer*; Jaehne, B., Monahan, E.C., Eds.; AEON Verlag & Studio, Hanau, Germany, 1995; pp 785-800.
- (30) Raymond, P. A.; Cole, J. J. *Estuaries* **2001**, *24*, 312-317.
- (31) King, D.B.; Saltzman, E.S. *J. Geophys. Res.* **1995**, *100*, 7083-7088.
- (32) Jähne, B.; Münnich, K. O.; Bosinger, R.; Dutzi, A.; Huber, W.; Libner, P. J. *J. Geophys. Res.* **1987**, *92*, 1937-1949.
- (33) Smith, R. *J. Hydraul. Eng.* **1998**, *124*, 117-122.
- (34) Purnama, A.; Kay, A. *Environmetrics* **1999**, *10*, 601-624.

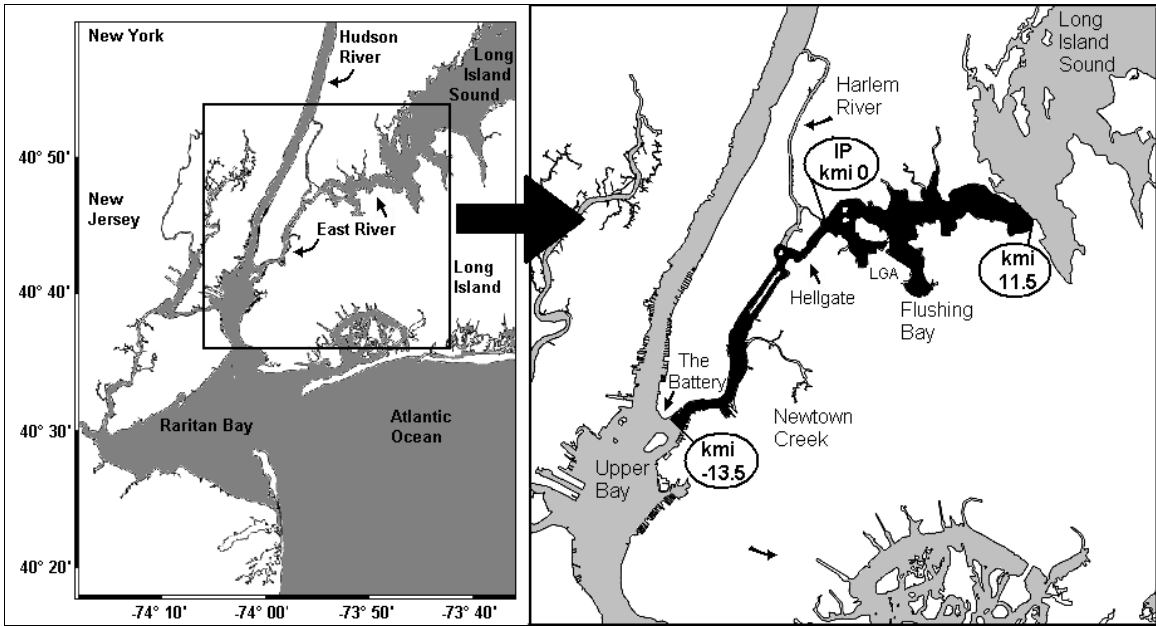


Figure 1: Overview of the East River (filled in black), showing SF<sub>6</sub> injection location (IP) and river endpoints. Points on the East River are referenced by kmi, the distance in km from the IP.

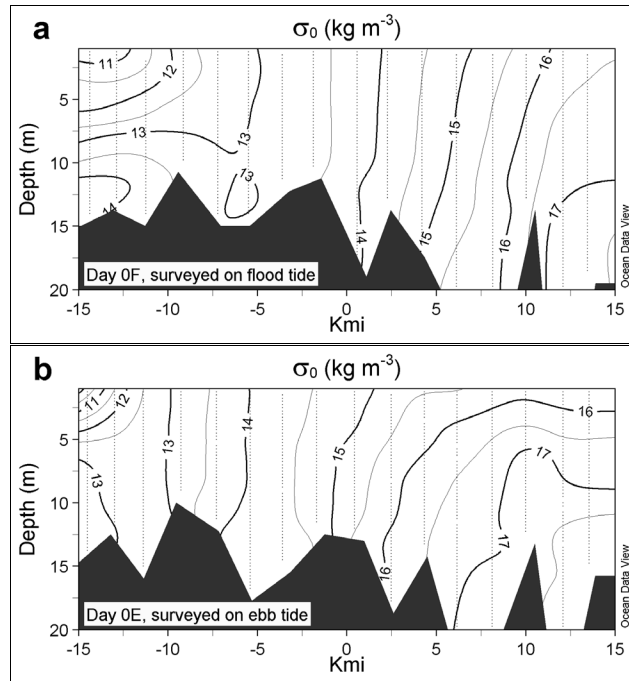
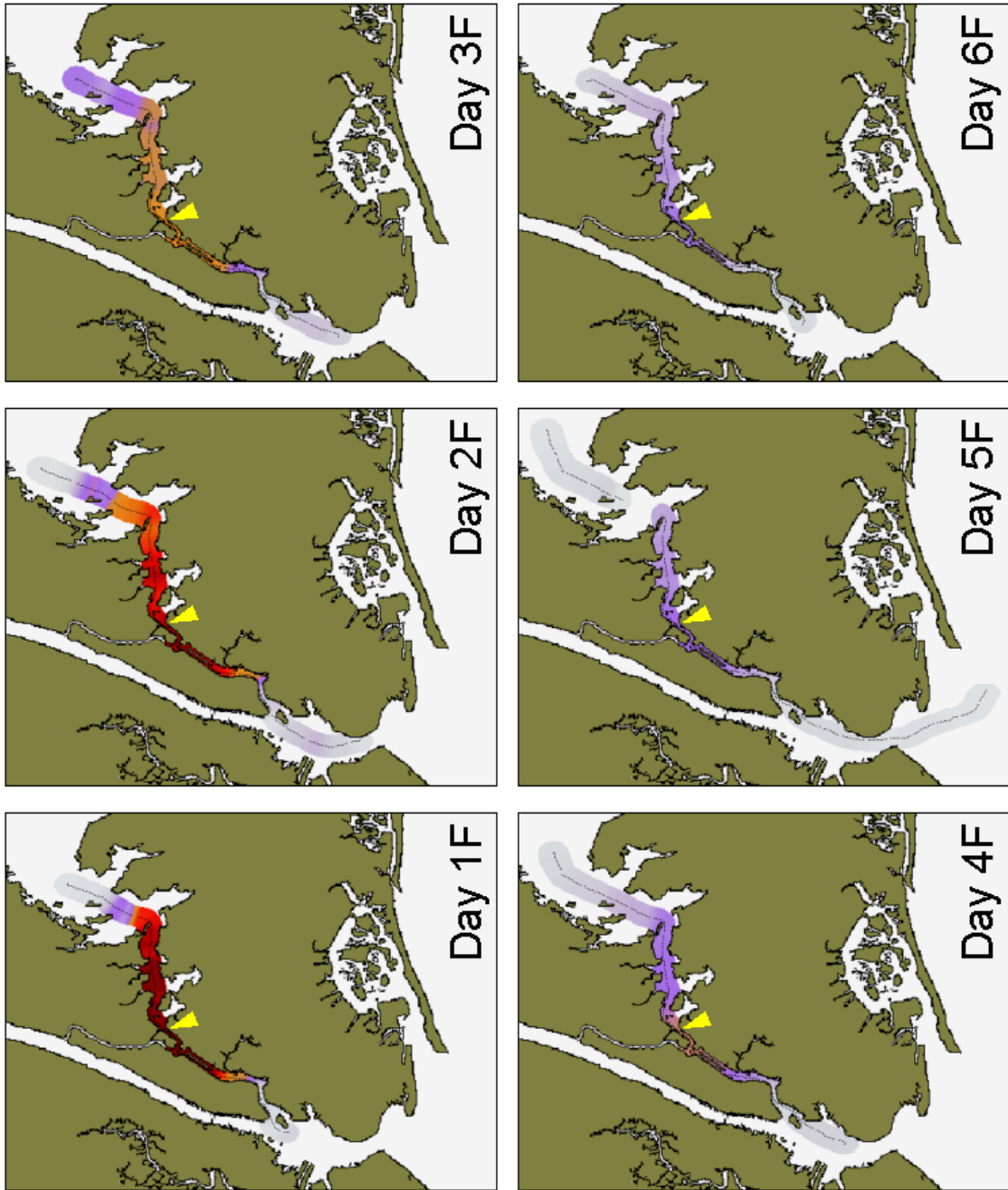


Figure 2: Longitudinal sections of potential density ( $\sigma_0$ ) in the East River from CTD surveys on (a) day 0F (June 17, 2003) and (b) day 0E (June 25, 2003). The surveys passed from Upper Bay to Long Island Sound, began 2 h after SBF on Day 0F and 2 h after SBE on Day 0E, and lasted 3 h. Lines of small dots indicate sample points. A consistent structure is evident in the 2 surveys, displaced by the tide.

(a)



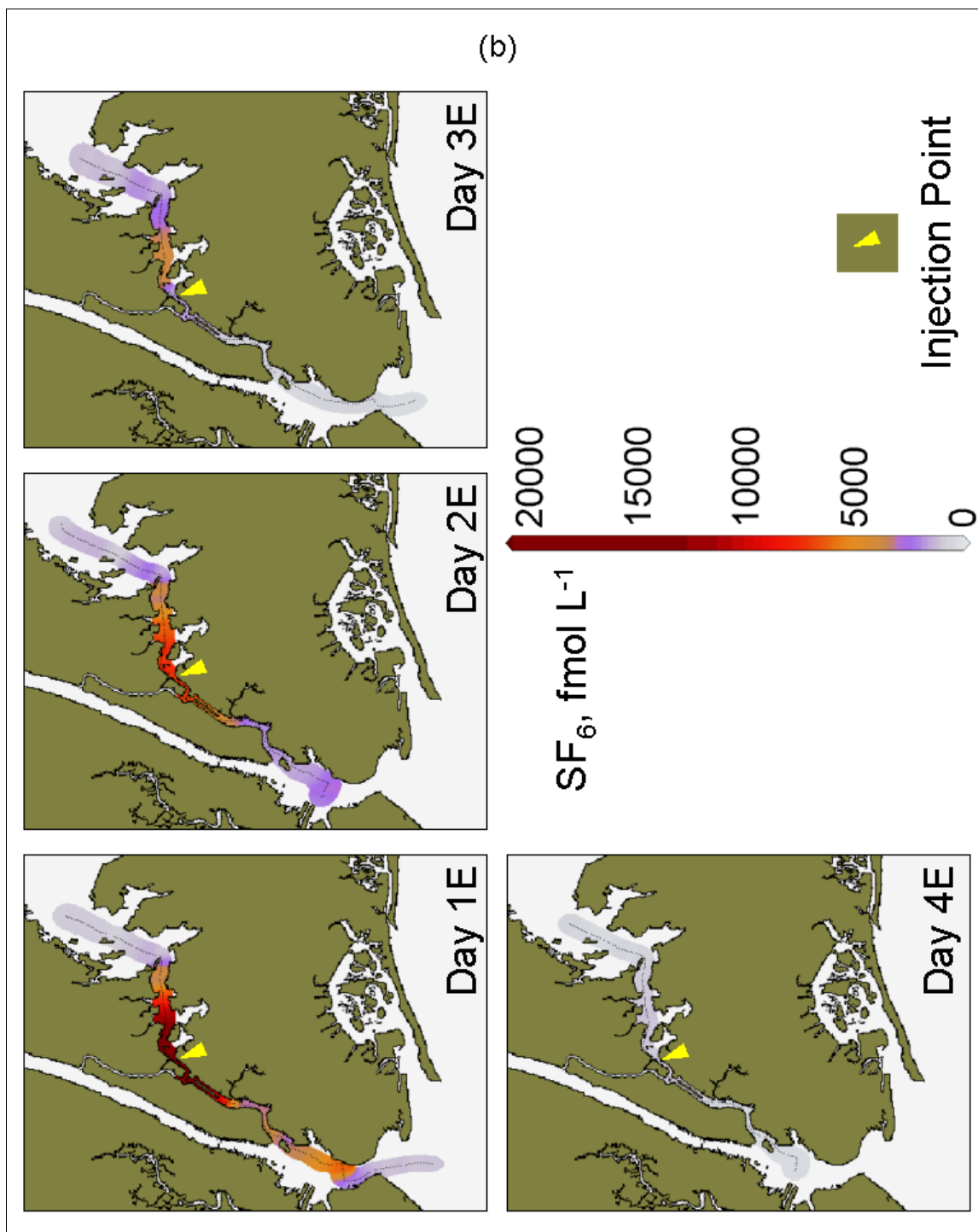


Figure 3: Tidally synchronized longitudinal surveys of measured  $\text{SF}_6$  concentrations in the East River for (a) 6 days following the injection at SBF (days 1F–6F), and (b) 4 days following the injection at SBE (days 1E–4E). Sample points are shown by strings of small black dots.

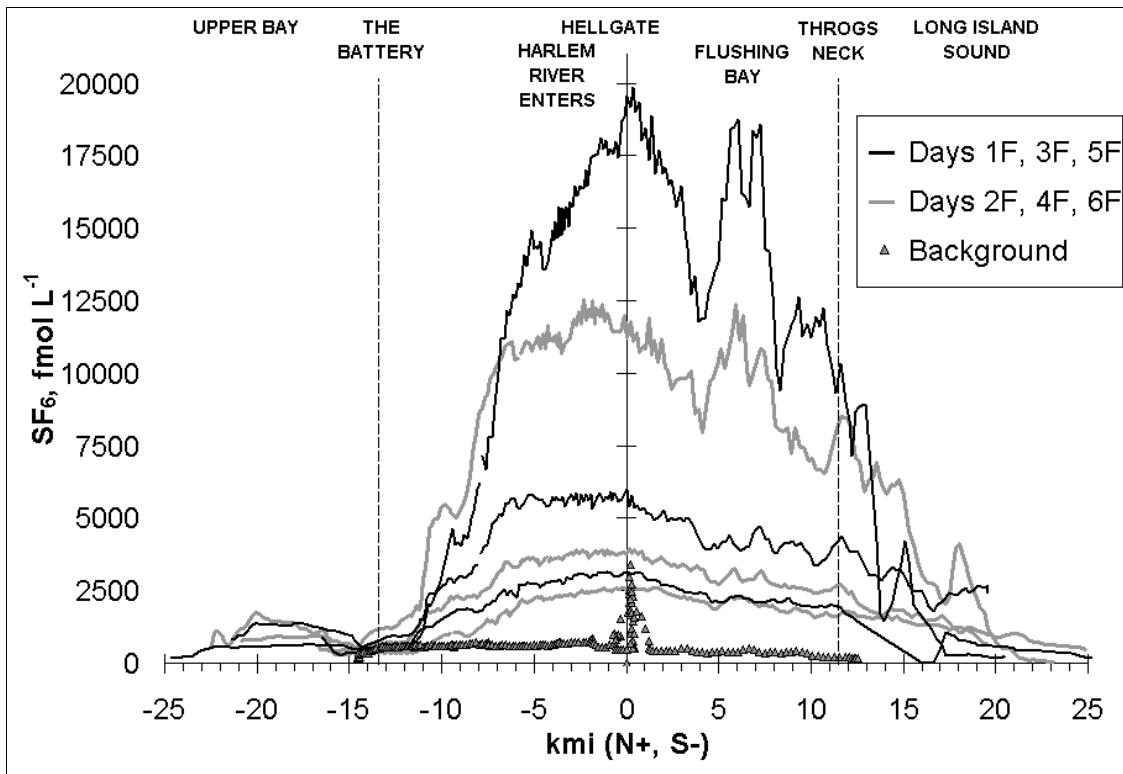


Figure 4: Tidally synchronized  $SF_6$  surveys in the East River for 6 days (day 1F to day 6F) following the injection at SBF at kmi 0 on day 0F. The two dashed lines denote the two ends of the East River. A background survey from the day before the flood injection exhibits a spike near the injection point; the exact source of this spike was searched for but not discovered.

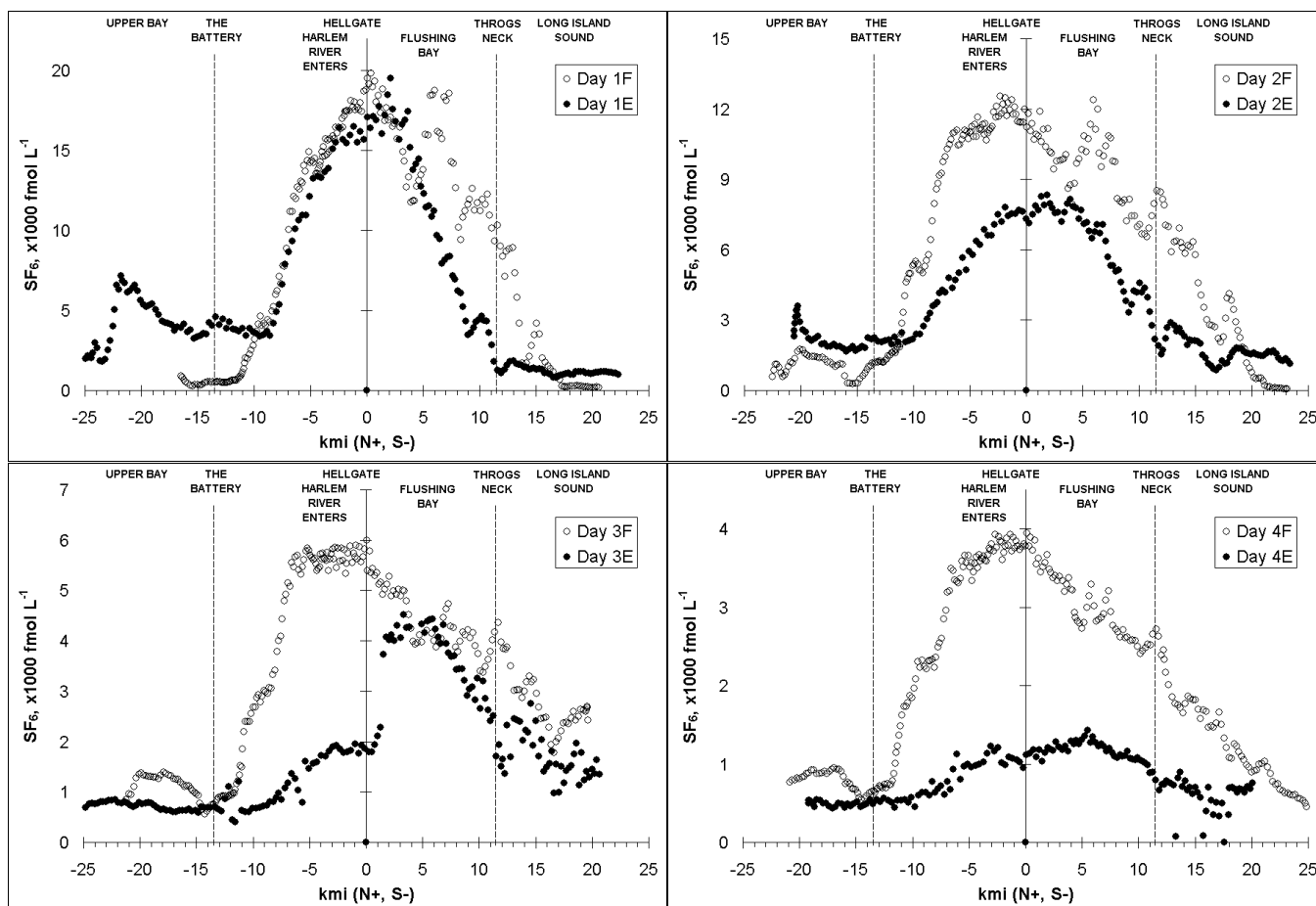


Figure 5: Comparisons of tidally synchronized SF<sub>6</sub> surveys in the East River following the flood (open circles; measured at SBF) and ebb injections (closed circles; measured at SBE). Differential flushing of the tracer as a function of tidal phase during injection is clearly evident. A large pulse of tracer is exhibited in Upper Bay on day 1E, indicating a loss pathway that depresses concentrations relative to the flood injection, first in lower half of the river (days 2E–3E), and then throughout the study area (day 4E). Both series of surveys manifest a persistent sharp drop at or above the Battery, indicating strong dispersive mixing in Upper Bay.

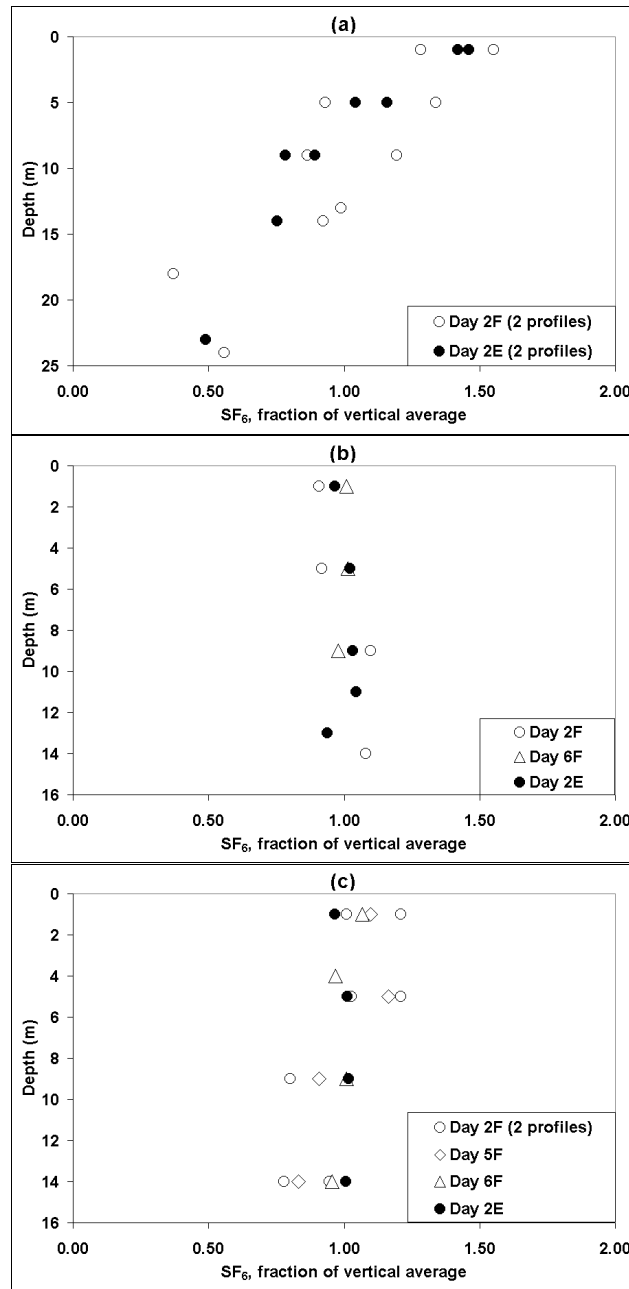


Figure 6: Vertical profiles of SF<sub>6</sub> concentrations in the East River from three regions: (a) upper half of the river; (b) injection point; (c) lower half of the river. The vertical structure in the lower half of the river and at the injection point is weak, but in the upper half of the river, a strong gradient is evident that depends upon neither the tidal phase of the injection nor the tidal phase of the data collection.

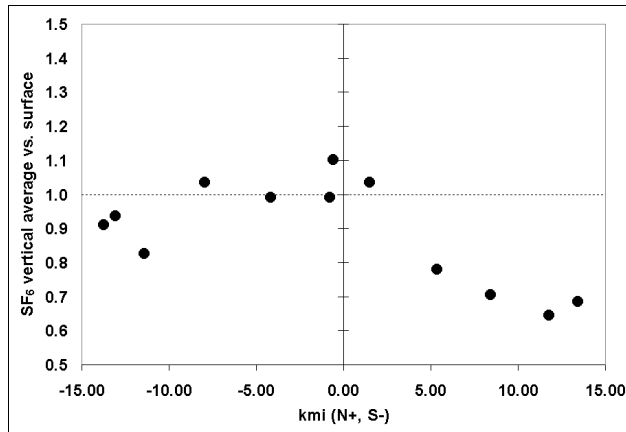


Figure 7: Longitudinal distribution of correction factors for estimating mean water column tracer concentration in the East River from observations of surface concentrations. The points shown are compiled from vertical profiles taken at different states of the tide on 4 separate days (see Figure 6).

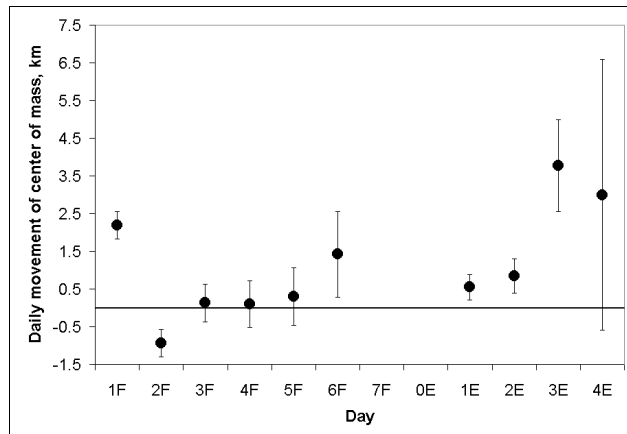


Figure 8: Movement of the center of mass (COM) of  $\text{SF}_6$  in the East River. The COM of the  $\text{SF}_6$  background has been subtracted.

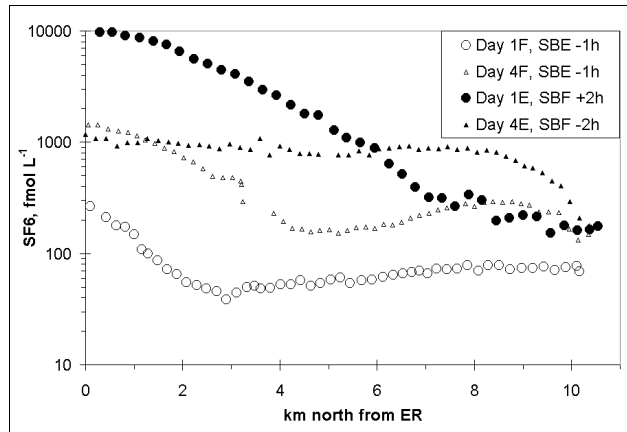


Figure 9: Longitudinal surveys of SF<sub>6</sub> in the Harlem River 1 and 4 days following the flood and ebb injections in the East River. The ebb injection produced much higher tracer levels in the Harlem River, an effect that persisted at least 4 days, despite flushing of this injection from the ER at twice the rate of the flood injection. Tidal phase at time of observation is indicated in the legend. Tidal excursion is ~11 km.

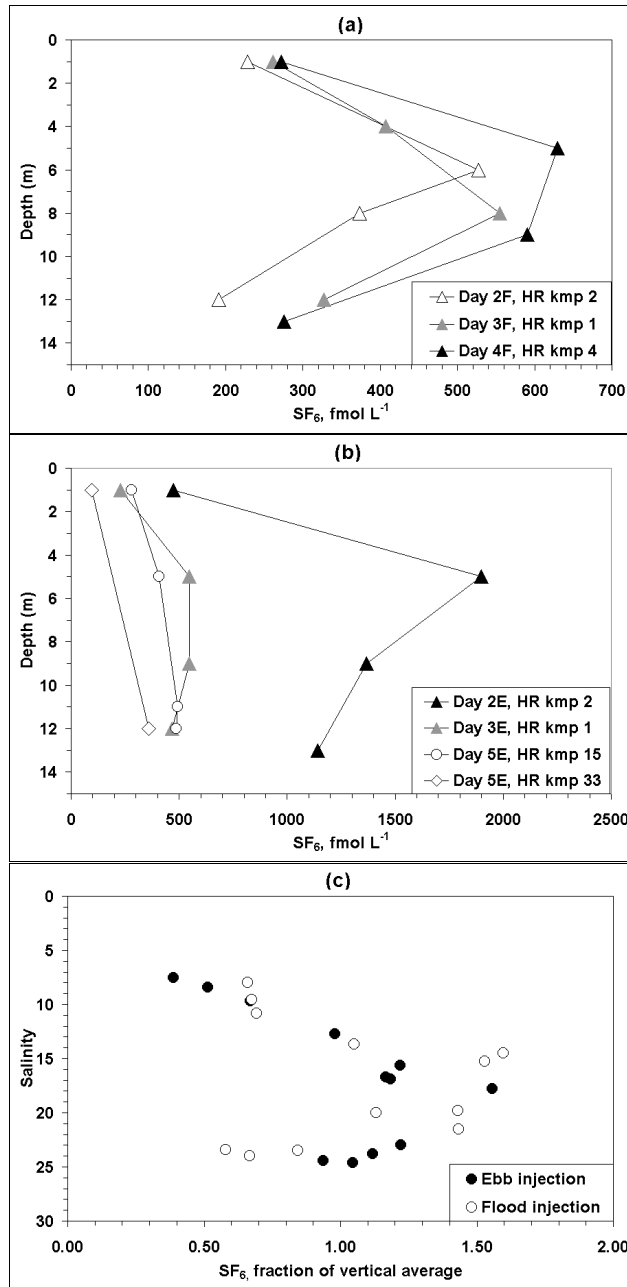


Figure 10: In (a) and (b), vertical SF<sub>6</sub> profiles in the Hudson River following the flood and ebb injections, respectively. Distance north of the Battery is indicated as “HR kmp”. In (c), normalized SF<sub>6</sub> concentrations plotted against salinity for the combined set of profiles. The peak SF<sub>6</sub> concentrations are found in an intermediate water layer, at salinities matching those in the East River.

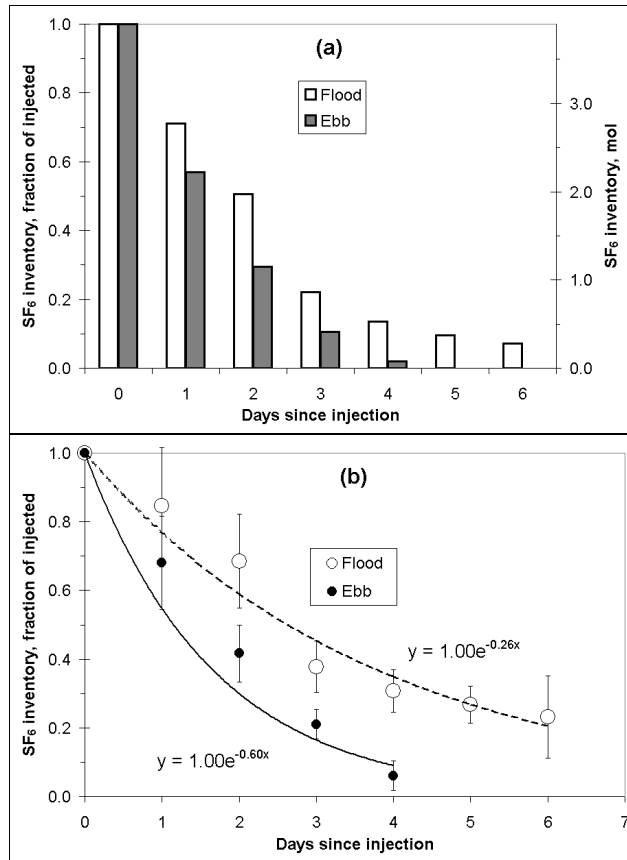


Figure 11: Decay of the SF<sub>6</sub> mass inventory in the East River after the flood and ebb injections. In (a), measured mass inventories (raw data) plotted against time. In (b), the same data after removing the estimated effects of gas exchange; this figure represents the expected behavior of nonvolatile and/or particle-bound contaminants. Fitted exponential decay curves are shown, defining a mean residence time. For the ebb injection, the curve fit is somewhat crude, but matches the inventory reasonably well on days 3E and 4E.